OPEN

Comparison of the Sensitivity and Specificity of 5 Image Sets of Dual-Energy Computed Tomography for Detecting First-Pass Myocardial Perfusion Defects Compared With Positron Emission Tomography

Wenhuan Li, MD, Xiaolian Zhu, MS, Jing Li, MD, Cheng Peng, MD, Nan Chen, MD, Zhigang Qi, MD, Qi Yang, MD, Yan Gao, MD, Yang Zhao, MS, Kai Sun, MD, and Kuncheng Li, MD, PhD

Abstract: The sensitivity and specificity of 5 different image sets of dual-energy computed tomography (DECT) for the detection of first-pass myocardial perfusion defects have not systematically been compared using positron emission tomography (PET) as a reference standard.

Forty-nine consecutive patients, with known or strongly suspected of coronary artery disease, were prospectively enrolled in our study. Cardiac DECT was performed at rest state using a second-generation 128-slice dual-source CT. The DECT data were reconstructed to iodine maps, monoenergetic images, 100 kV images, nonlinearly blended images, and linearly blended images by different postprocessing techniques. The myocardial perfusion defects on DECT images were visually assessed by 5 observers, using standard 17-segment model. Diagnostic accuracy of 5 image sets was assessed using nitrogen-13 ammonia PET as the gold standard. Discrimination was quantified using the area under the receiver operating characteristic curve (AUC), and AUCs were compared using the method of DeLong.

The DECT and PET examinations were successfully completed in 30 patients and a total of 90 territories and 510 segments were analyzed. Cardiac PET revealed myocardial perfusion defects in 56 territories (62%) and 209 segments (41%). The AUC of iodine maps, monoenergetic images, 100 kV images, nonlinearly blended images, and linearly blended images were 0.986, 0.934, 0.913, 0.881, and 0.871, respectively, on a per-territory basis. These values were 0.922, 0.813, 0.779, 0.763, and 0.728, respectively, on a per-segment basis.

DECT iodine maps shows high sensitivity and specificity, and is superior to other DECT image sets for the detection of myocardial perfusion defects in the first-pass myocardial perfusion.

(*Medicine* 93(28):e329)

Abbreviations: ^{13}N = nitrogen-13, AUC = area under the ROC curve, CAD = coronary artery disease, CCTA = coronary computed tomography angiography, CI = confidence interval, DECT = dual-energy computed tomography, DSCT = dual-source CT, NPV = negative predictive value, PET = positron emission tomography, PPV = positive predictive value, SPECT = single photon emission computed tomography.

INTRODUCTION

Myocardial infarction is a direct cause of morbidity and mortality in patients with coronary artery disease (CAD).[1] It is known that a significant number of patients experiencing an acute myocardial infarction have normal coronary arteries or nonsignificant coronary stenosis at invasive coronary angiography, because reduction of myocardial blood supply may be caused by microvascular dysfunction or disruption of a mild vulnerable plaque.[2] Current guidelines have shown that comprehensive and accurate assessment of coronary stenosis and myocardial perfusion is crucial to risk stratification and therapeutic planning in patients with CAD.[3,4]

Single photon emission computed tomography (SPECT) and positron emission tomography (PET) are established and most commonly used in myocardial perfusion imaging.[4,5] However, SPECT and PET have the disadvantages of relatively low spatial resolution and being unable to supply coronary artery anatomical information simultaneously. Coronary computed tomography angiography (CCTA) is a well-established noninvasive imaging modality for the plaque detection, even in the mild atherosclerotic plaque not affecting the coronary lumen because of outward remodeling.[4,6,7] With the improvement in equipment and technology, CT can be used for perfusion imaging.[8] Currently, 2 different CT-based approaches are used for myocardial perfusion. One is dynamic perfusion technique, time-resolved image acquisition at multiple time points during the passage of a contrast medium bolus through the myocardium. However, the disadvantage of this technique is requiring 2 separate (CCTA and dynamic myocardial perfusion) scans, which increases additional scan time, iodine contrast, and radiation exposure. The second approach is first-pass myocardial perfusion, a static image reflecting myocardial blood pool at the early arterial phase.[9]

CT myocardial perfusion is susceptible to beam-hardening artifacts from conventional single-energy CT scanning, which can mimic perfusion defects.[10] Recent studies have shown that different first-pass dual-energy CT (DECT) image sets have different potential to eliminate beam hardening and improve the contrast resolution by different postprocessing techniques.[11–15] But these studies just focus on evaluating 1 or a few image sets of DECT, and no studies have systematically compared diagnostic performance of all the DECT image sets. Thus, the

Editor: Xiaowen Hu.
Received: June 29, 2014; revised: November 7, 2014; accepted: November 11, 2014.
From the Department of Radiology (WL, XZ, NC, ZQ, QY, YG, YZ, KS, KL); Department of Cardiology (JL); and PET Centre (CP), Xuanwu Hospital of Capital Medical University, Beijing, China.
Correspondence: Kuncheng Li, MD, Xuanwu Hospital of Capital Medical University, No. 45 Chang Chun Street, Xi Cheng District, Beijing 100053, China (e-mail: kuncheng.li@hotmail.com).
This study was supported by the National Basic Research Program of China (973 Program, No. 303-01-001-0018).

ISSN: 0025-7974
DOI: 10.1097/MD.0000000000000329

purpose of our study was to systematically compare diagnostic accuracy of 5 different DECT image sets (iodine maps, monoenergetic images, 100 kV images, nonlinearly blended images, and linearly blended images) and identify the optimal DECT image set for the detection of myocardial perfusion defects in first-pass myocardial perfusion. Furthermore, our study chose nitrogen-13 (^{13}N) ammonia PET as the reference standard, which is different from previous studies, because PET is superior to SPECT.[4,16]

MATERIALS AND METHODS

Study Population

Our study was approved by the institutional ethics committee, and the written informed consent was obtained from each patient. From March 2013 to October 2014, 49 consecutive patients with known or strongly suspected CAD, who were referred for cardiac CT evaluation at Xuanwu Hospital, Beijing, China, were prospectively enrolled in our study. Patients underwent first-pass cardiac DECT scan within 1 week before or after ^{13}N-ammonia PET examination. Patients with known renal insufficiency (serum creatinine level >1.5 mg/dL [132.6 μmol/L]), contrast media allergy, atrial fibrillation or other heart rhythm irregularity, and inability to perform breath holding were excluded.

Three patients did not undergo DECT examination because of renal insufficiency (n = 1), contrast allergy (n = 1), or atrial fibrillation (n = 2). Eight patients did not undergo PET examination because of withdrawal of consent (n = 10) or transfer to another hospital (n = 5). The DECT and PET examinations were successfully completed in 30 of 49 patients.

DECT Scan Protocol

All DECT examinations were performed at resting state using a second-generation 128-slice dual-source CT (DSCT) (SOMATOM Definition Flash, Siemens Healthcare, Forchheim, Germany). All scanning parameters of the dual-energy mode were as follows: 280 milliseconds rotation time, $2 \times 64 \times 0.6$ mm acquisition collimation with z-flying focal spot technique, and heart rate adaptive pitch of 0.17 to 0.35. Automated tube current modulation (Care Dose 4D, Siemens Healthcare) was used. One tube of DSCT system was operated with 165 reference mAs per rotation at 100 kV, and the second tube was automatically operated with 140 reference mAs per rotation at 140 kV. DECT was performed using a retrospective electrocardiographic gating with electrocardiogram-dependent tube current modulation scan protocol (full-dose window during 30%–80% phases of the cardiac cycle). Before the examination, each patient's heart rate was measured. If the patient's resting heart rate was >65 beats per minute and no contraindication to the use of β-blockers, metoprolol tartrate (Beloc, AstraZeneca, Wedel, Germany) was administered intravenously in fractions of 5 to 25 mg before the examination. All scans were performed in craniocaudal direction of supine position during a mid-inspiratory breath-hold. The scanning range started from above the origin of the coronary arteries to below the dome of the diaphragm. Contrast agent was injected by a dual-syringe injector (Stellant D, Medrad, Indianola, PA) using an 18-gauge intravenous needle placed in the right antecubital vein. A triphasic injection protocol was used.[17] First, 50 mL of pure contrast media (Iopromide, Ultravist 370, 370 mg/mL; Bayer-Schering Pharma, Berlin, Germany) was administered. Thereafter, 30 mL of a 70%/30% saline/contrast medium mixture was administered. Finally, 30 mL of saline was administered. The injection rates for all phases were 5 mL/s. Contrast agent application was controlled by a bolus-tracking technique. A region of interest was placed in the aortic root, and image acquisition was automatically started 7 seconds after the signal attenuation reached the predefined threshold of 100 Hounsfield units.

Image Postprocessing and Analysis for DECT

DECT images were reconstructed using Best Phase technique (Best Phase; Siemens Healthcare) from raw data, with 280 milliseconds temporal resolution, 1.5 mm slice thickness, 1.0 mm increment, and a dedicated dual-energy convolution kernel (D30f). By default, raw data were automatically reconstructed into 3 separate image sets: low-kilovoltage (100 kV), high-kilovoltage (140 kV), and linearly blended image sets. The linearly blended images used a weighting factor of 0.3, combining 30% of 100 kV data and 70% of 140 kV data.[14] Then the 100 and 140 kV image sets were transferred to multimodality workplace (MMWP; Siemens Healthcare) and loaded into the dual-energy application. In the dual-energy application, the nonlinearly blended (Optimum Contrast) images were obtained by choosing the Optimum Contrast application class. The nonlinear blending center and width were set to 110 and 0, respectively.[18] Monoenergetic images were obtained by choosing the Monoenergetic application class, and the energy value of monoenergetic images was set to 70 keV in our study.[19,20] Iodine maps were obtained by choosing heart perfusion blood volume (Heart PBV) application class. The attenuation of epicardial fat in 100 and 140 kV image sets were measured and used for calibration of the heart perfusion blood volume algorithm. The iodine maps were superimposed as a 70% overlay onto grayscale (virtual noncontrast images), with color-coded of ''Hot Body 8 bit.'' Areas of normal myocardial perfusion were chosen to normalize the iodine maps.[9] Figure 1 shows DECT image postprocessing and Figure 2 shows all DECT resulting image sets (iodine maps, monoenergetic images, 100 kV images, nonlinearly blended images, and linearly blended images) reconstructed for each patient.

All DECT images were assessed on MMWP workstation in a quiet environment. All DECT images were visually assessed independently by 5 cardiac radiologists (W.L., X.Z., N.C., Q.Y., and Y.G.), with 6, 10, 22, 18, and 13 years of experience in cardiac imaging, respectively, who were unaware of clinical data and results of other imaging findings. All DECT images were assessed on a per-territory and segment basis according to the American Heart Association 17-segment model.[21] At each time,1 territory or segment was randomly selected and evaluated, taking about 30 seconds (one territory) and 10 seconds (one segment), respectively. Before evaluating, patient information was removed, with single image presented on a computer screen. For grayscale images, normal myocardium was defined as homogeneous enhancement without any area of hypoattenuation; myocardial perfusion defect was defined as distinct hypoattenuation compared with normal surrounding myocardium. For color-coded iodine maps, light orange indicated the highest iodine content and gray indicated the absence of iodine.

PET Data Acquisition

All PET examinations were performed at rest on ECAT EXACT (CTI-Siemens, Knoxville, TN), which provide 47 tomographic slices. All patients were advised to fast for at

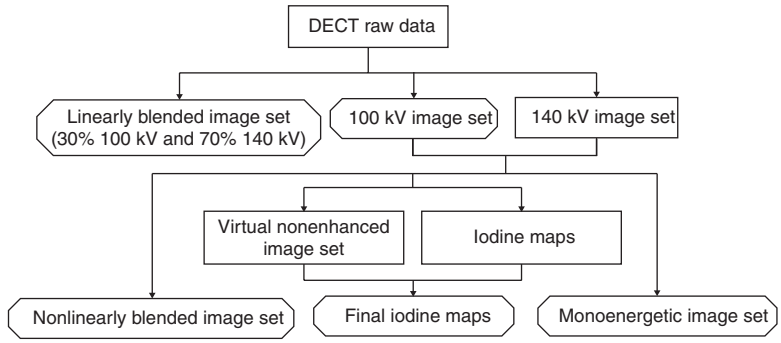

FIGURE 1. DECT image data processing. Based on a single dual-energy CT acquisition, 3 different image sets were reconstructed from raw data; reconstructed original image sets (100 and 140 kV) were reformatted to nonlinearly blended images, final iodine maps, and monoenergetic images by different image-processing strategies. DECT = dual-energy computed tomography.

least 6 hours before the PET examination. PET myocardial blood flow imaging was performed 5 minutes after 15 mCi ^{13}N-ammonia was injected. The data acquisition time for PET imaging was 30 minutes. Tomographic images were reconstructed by the filtered back projection method. Typical horizontal long axis, vertical long axis, and short axis tomographic views of the left ventricle were obtained by an image-processing workstation for image analysis.

Statistical Analysis

All statistical analyses were performed using SAS version 9.1 (SAS Institute Inc, Cary, NC), and statistical significance was determined by a P value <0.05.

The diagnostic performances of 5 different DECT image sets for the detection of myocardial perfusion defects (sensitivity, specificity, positive predictive value [PPV], negative predictive value [NPV], and accuracy with 95% confidence intervals) were calculated. Discrimination of 5 different DECT image sets was quantified using the area under curve (AUC), and AUCs were compared using the method of DeLong.[22,23] Kappa test was calculated to check the agreement between the results of the 2 observers. The κ value was interpreted as follows: 0 to 0.20 poor agreement, 0.21 to 0.40 fair agreement, 0.41 to 0.60 moderate agreement, 0.61 to 0.8 good agreement, and >0.81 excellent agreement.

RESULTS

The characteristics of the study population are summarized in Table 1. For the first-pass DECT scanning, the mean estimated radiation effective dose was 4.74 ± 0.8 mSv (dose-length product × 0.014 mSv/mGy·cm).

The image qualities of 30 patients were good enough for further analysis and a total of 90 myocardial territories and 510 myocardial segments were evaluated. Cardiac PET revealed myocardial perfusion defects in 56 territories (62%) and 209 segments (41%). The AUC of iodine maps, monoenergetic images, 100 kV images, nonlinearly blended images and linearly blended images were 0.986, 0.934, 0.913, 0.881, and 0.871, respectively, on a per-territory basis (Figure 3A). These values were 0.922, 0.813, 0.779, 0.763, and 0.728, respectively, on a per-segment basis (Figure 3B). For the comparisons of every 2 AUCs, the significance levels (P values) were shown in Figure 3. Sensitivity, specificity, PPV, NPV, and accuracy of 5 reconstruction image sets for the detection of myocardial perfusion defects were summarized in Table 2. Interobserver agreement for the detection of myocardial perfusion defects on iodine maps, monoenergetic images, and nonlinearly blended images was excellent ($k = 0.96$, 0.82, and 0.84, respectively), and interobserver agreement on 100 kV images and linearly blended images was good ($k = 0.76$ and 0.73, respectively), with all P value <0.001.

DISCUSSION

In cardiac DECT, different postprocessing strategies can produce different image sets that have different advantages in improving diagnostic accuracy by increasing contrast-to-noise ratio (CNR), signal-to-noise ratio (SNR), and reducing beam-hardening artifacts.[9,14,18,19,24] By comparing the diagnostic value of different DECT image sets, we found that DECT iodine maps showed better diagnostic accuracy compared to monoenergetic images, 100 kV images, nonlinearly blended images, and linearly blended images in first-pass myocardial perfusion, on a per-segment and per-territory basis.

A recent study, comparing iodine maps, linearly blended images (30% 100 kV and 70% 140 kV) and 100 kV images, also demonstrated that iodine maps had better diagnostic performance than linearly blended images and 100 kV images, for the detection of myocardial perfusion defects on SPECT.[14] This may be because material decomposition strategy used in iodine maps is more suitable than blending of the low and high-kilovolt and monoenergetic techniques used in other image sets, for the detection of myocardial perfusion defects in first-pass DECT, whereas blending of the low and high-kilovolt and monoenergetic images have an optimal balance of maximally increasing attenuation and decreasing noise with a consequently increase in CNR and SNR. Contrary to first-pass DECT, blending images of the low and high kilovolt show more advantages than iodine maps in late-phase DECT for visualization of delayed myocardial contrast enhancement of DECT in acute myocardial infarction.[24]

Actually, 100 kV image set is equal to linearly blended image set with weighting factor of 0 (100% of 100 kV data and 0% of 140 kV data). The biggest difference between linearly blended images and nonlinearly blended images is that each pixel may have different mixing ratio in nonlinearly blended images to get optimal contrast for every pixel, whereas linearly blended images have same mixing ratio in every pixel. Holmes et al[25] found that nonlinearly blended images had a higher CNR and more conspicuous than the standard 0.3 linearly blending

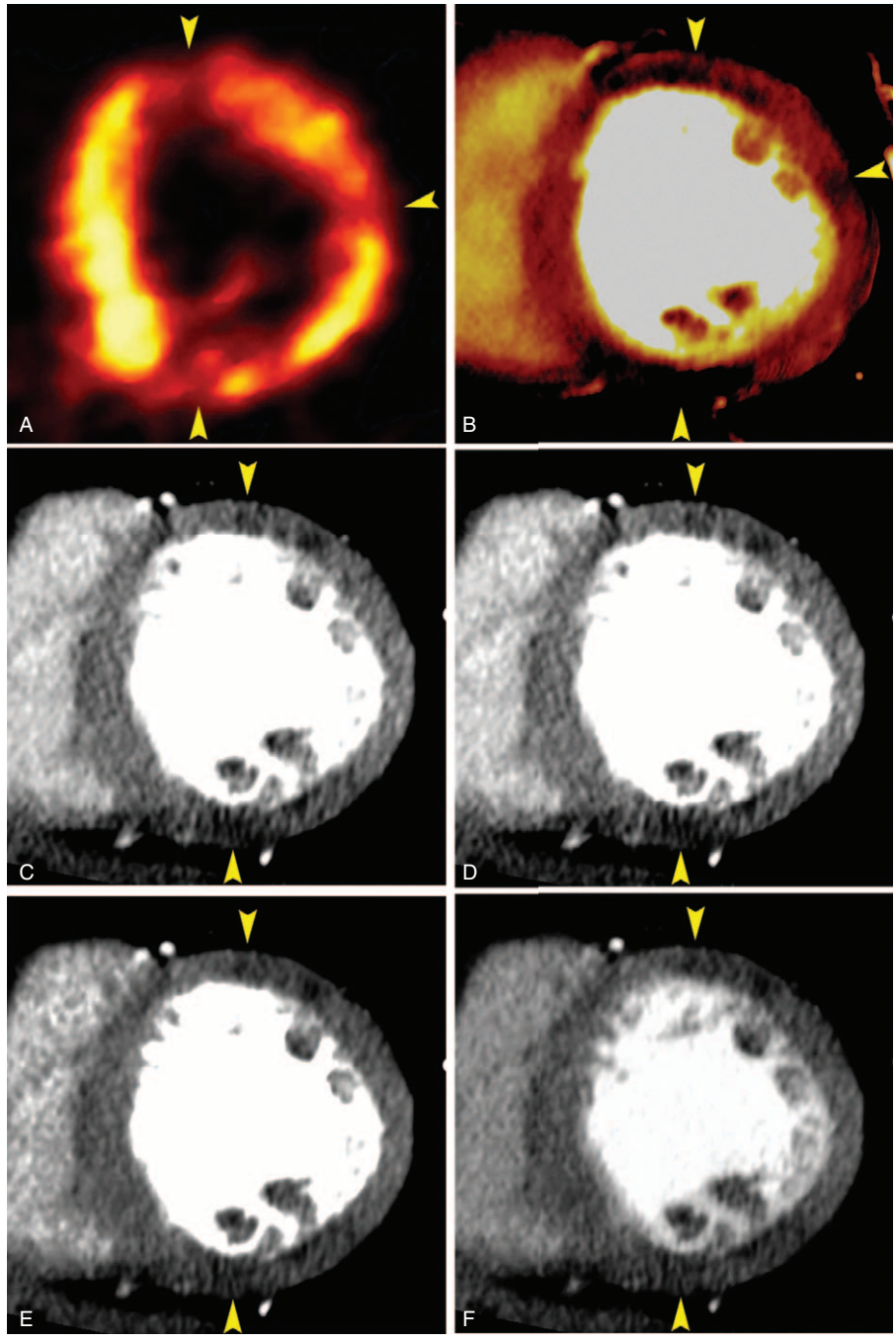

FIGURE 2. A 64-year-old man with hypertension, dyslipidemia, underwent imaging because of paroxysmal chest distress for 1 year. PET (A) short-axis image shows myocardial perfusion defects in anterior, anterolateral, and inferior wall (yellow arrows). Iodine map (B) shows good correlation with PET image. Monoenergetic image (C), 100 kV image (D), nonlinearly blended image (E), and linearly blended image (F) do not clearly show anterolateral myocardial blood volume deficits, and only moderately show myocardial perfusion defects in anterior and inferior wall (yellow arrows). Figure 2C to F is shown with identical window setting (center, 105 HU; width, 120 HU). HU = Hounsfield units, PET = positron emission tomography.

images on liver visual analysis. Our study suggests that such result can also apply to first-pass DECT myocardial perfusion.

Diagnostic accuracy of iodine maps in our study is higher (90.0%) than previous studies (85%–88% on a per-segment basis).[14,17] This may be because previous studies evaluating DECT iodine maps all used SPECT as the reference standard. Our study used ^{13}N-ammonia PET as the gold standard. As is known to all, PET has higher spatial resolution and contrast resolution compared to SPECT that increased sensitivity for the detection of myocardial perfusion defects. In addition, PET has a more robust attenuation correction than SPECT. This property affords PET more specificity compared to SPECT, particularly

TABLE 1. Characteristics of the Study Population (n = 30 Patients)

Characteristics	Value
Age, y, (mean ± SD; range)	57 ± 11 (39, 81)
Sex (male/female)	15/15
BMI, kg/m^2 (mean ± SD; range)	23 ± 3 (20, 31)
Mean heart rate during DECT, bpm (mean ± SD; range)	59 ± 11 (45, 82)
Hypertension, %	10 (33%)
Hypercholesterolemia, %	12 (40%)
Diabetes mellitus, %	9 (30%)
Current or prior cigarette smoking, %	7 (23%)

Values are n (%). BMI = body mass index, bpm = beats per minute, DECT = dual-energy computed tomography, SD = standard deviation.

for obese patients or females, where a breast attenuation artifact can lead to a false-positive result.[26]

A recent study demonstrated that 45% reversible perfusion defects at SPECT were detected by DECT iodine maps at rest.[15] The fact that resting DECT iodine maps can identify reversible perfusion defects that are visible only on stress SPECT is also reported in other literatures.[9,17,27] This phenomenon may be related to different factors. The spatial resolution of DECT is superior to SPECT or PET and may allow detection of smaller, especially subendocardial perfusion defects that are not noticed on rest SPECT or PET. Furthermore, the iodine contrast medium, as used in CT, is considered to have a vasodilatory effect that may cause a degree of hyperemia such as the response to vasodilator drugs in myocardial perfusion imaging. Last, different distribution kinetics of the different contrast agents in myocardium enable CT to detect more subtle reductions in myocardial perfusion compared with SPECT or PET.[9,28]

Currently, increasing attention is being paid to the radiation dose for cardiac CT application. In this study, although the DECT and PET were performed for each patient, it does not increase the radiation dose obviously. This is because of 2 reasons. First, compared with the routine use of retrospectively ECG-gated CCTA (9.83 ± 3.49 mSv), the DECT (4.74 ± 0.8 mSv) generated from dual-source CT does not come at a penalty of additional radiation dose but has a decrease in the radiation dose (Supplemental figure, http://links.lww.com/MD/A117), because the tube current for the 2 energy levels can be adapted in dual-source CT system.[9,29] Second, we used PET as the gold standard. The main advantage of the positron-emitting tracers is the shorter physical half-life compared to the SPECT tracers; therefore, the radiation burden to patients is relatively low.[26] For the cardiac PET examination, the radiation dose from 15 mCi (555 MBq) of ^{13}N-ammonia is 1.11 mSv (the conversion factor 0.002 mSv/MBq).[30]

Our study has several limitations that need to be discussed. First, the first-pass DECT and cardiac PET were performed at rest without pharmaceutical stress. Future studies need to explore the diagnostic potential of different DECT image sets for detecting myocardial perfusion defects at stress and rest. Second, the relatively small number of patients included in this study limits the statistical power and strength of the conclusion. Third, in view of the relatively small sample size, per-patient

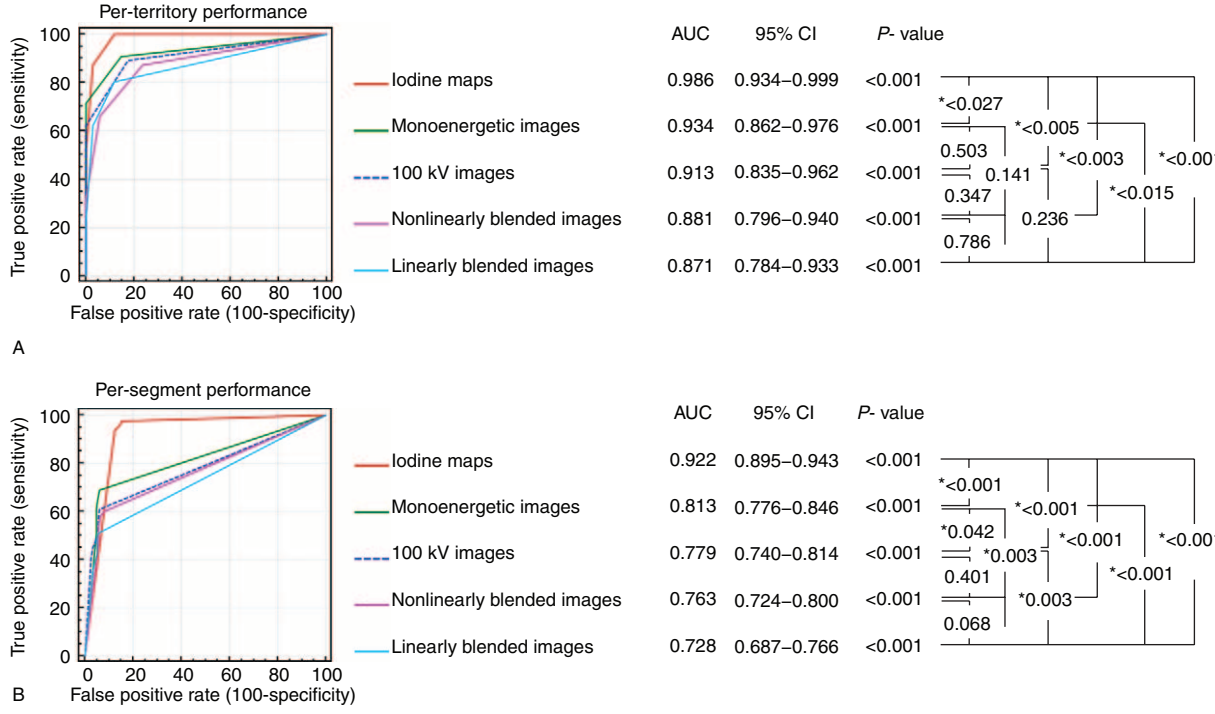

FIGURE 3. Receiver operating characteristic (ROC) curve with corresponding area under the curve (AUC) and 95% confidence interval (CI) describing the diagnostic performance of 5 DECT image sets, using PET as reference standard, on a per-territory (A) and segment (B) basis. $^*P < 0.05$ for comparison of AUC between image sets. DECT = dual-energy computed tomography.

TABLE 2. Statistical Results of Different DECT Image Sets

Image Sets	Accuracy	Sensitivity	Specificity	PPV	NPV
Per territory (n = 90)					
Iodine maps	91.1 (82/90) [83.2–96.1]	98.2 (55/56) [90.5–99.9]	79.4 (27/34) [62.1–91.3]	88.7 (55/62) [78.1–95.3]	96.4 (27/28) [81.7–99.9]
Monoenergetic images	86.7 (78/90) [77.9–92.9]	85.7 (48/56) [73.8–93.6]	88.2 (30/34) [72.6–96.7]	92.3 (48/52) [81.5–97.9]	79.0 (30/38) [62.7–90.5]
100 kV images	82.2 (74/90) [72.7–89.5]	85.7 (48/56) [73.8–93.6]	76.5 (26/34) [58.8–89.3]	85.7 (48/56) [73.8–93.6]	76.5 (26/34) [58.8–89.3]
Nonlinearly blended images	80.0 (72/90) [70.3–87.7]	71.4 (40/56) [57.8–82.7]	94.1 (32/34) [80.3–99.3]	95.2 (40/42) [83.8–99.4]	66.7 (32/48) [51.6–79.6]
Linearly blended images	77.8 (70/90) [67.8–85.9]	69.6 (39/56) [55.9–81.2]	91.2 (31/34) [76.3–98.1]	92.9 (39/42) [80.5–98.5]	64.6 (31/48) [49.5–77.8]
Per segment (n = 510)					
Iodine maps	90.0 (459/510) [87.1–92.5]	97.6 (204/209) [94.5–99.2]	84.7 (255/301) [80.2–88.6]	81.6 (204/250) [76.2–86.2]	98.1 (255/260) [95.6–99.4]
Monoenergetic images	83.5 (426/510) [80.0–86.6]	68.9 (144/209) [62.2–75.1]	93.7 (282/301) [90.3–96.2]	88.3 (144/163) [82.4–92.8]	81.3 (282/347) [76.8–85.2]
100 kV images	80.4 (410/510) [76.7–83.8]	61.2 (128/209) [54.3–67.9]	93.7 (282/301) [90.3–96.2]	87.1 (128/147) [80.6–92.0]	77.7 (282/363) [73.1–81.9]
Nonlinearly blended images	79.0 (403/510) [75.2–82.5]	60.3 (126/209) [53.3–67.0]	92.0 (277/301) [88.4–94.8]	84.0 (126/150) [77.1–89.5]	76.9 (277/360) [72.2–81.2]
Linearly blended images	76.7 (391/510) [72.8–80.3]	50.7 (106/209) [43.7–57.7]	94.7 (285/301) [91.5–96.9]	86.9 (106/122) [79.6–92.3]	73.5 (285/388) [68.7–77.8]

Data are % (raw data) [95% confidence interval]. DECT = dual-energy computed tomography, NPV = negative predictive value, PPV = positive predictive value.

analysis was not performed. A potential limitation of per-segment analysis is that segments within the same coronary distribution might not be truly independent. Fourth, we did not correlate the results of DECT myocardial perfusion analysis with the results of CCTA.

In conclusion, DECT iodine maps shows high sensitivity and specificity, and is superior to other DECT image sets for the detection of myocardial perfusion defects in the first-pass myocardial perfusion. Future studies involving larger numbers of patients will be necessary for the validation of our findings.

REFERENCES

1. Go AS, Mozaffarian D, Roger VL, et al. Heart disease and stroke statistics – 2014 update: a report from the American Heart Association. *Circulation.* 2014;129:e28–e292.
2. Aldrovandi A, Cademartiri F, Arduini D, et al. Computed tomography coronary angiography in patients with acute myocardial infarction without significant coronary stenosis. *Circulation.* 2012;126:3000–3007.
3. Patel MR, Dehmer GJ, Hirshfeld JW, et al. ACCF/SCAI/STS/AATS/AHA/ASNC/HFSA/SCCT 2012 appropriate use criteria for coronary revascularization focused update: a report of the American College of Cardiology Foundation Appropriate Use Criteria Task Force, Society for Cardiovascular Angiography and Interventions, Society of Thoracic Surgeons, American Association for Thoracic Surgery, American Heart Association, American Society of Nuclear Cardiology, and the Society of Cardiovascular Computed Tomography. *J Thorac Cardiovasc Surg.* 2012;143:780–803.
4. Wijns W, Kolh P, Danchin N, et al. Guidelines on myocardial revascularization. *Eur Heart J.* 2010;31:2501–2555.
5. Klocke FJ, Baird MG, Lorell BH, et al. ACC/AHA/ASNC guidelines for the clinical use of cardiac radionuclide imaging – executive summary: a report of the American College of Cardiology/American Heart Association Task Force on Practice Guidelines (ACC/AHA/ASNC Committee to Revise the 1995 Guidelines for the Clinical Use of Cardiac Radionuclide Imaging). *J Am Coll Cardiol.* 2003;42:1318–1333.
6. Miller JM, Rochitte CE, Dewey M, et al. Diagnostic performance of coronary angiography by 64-row CT. *N Engl J Med.* 2008;359:2324–2336.
7. Hamon M, Biondi-Zoccai GG, Malagutti P, et al. Diagnostic performance of multislice spiral computed tomography of coronary arteries as compared with conventional invasive coronary angiography: a meta-analysis. *J Am Coll Cardiol.* 2006;48:1896–1910.
8. Becker A, Becker C. CT imaging of myocardial perfusion: possibilities and perspectives. *J Nucl Cardiol.* 2013;20:289–296.
9. Vliegenthart R, Pelgrim GJ, Ebersberger U, et al. Dual-energy CT of the heart. *AJR Am J Roentgenol.* 2012;199:S54–S63.
10. Rodriguez-Granillo GA, Rosales MA, Degrossi E, et al. Signal density of left ventricular myocardial segments and impact of beam hardening artifact: implications for myocardial perfusion assessment by multidetector CT coronary angiography. *Int J Cardiovasc Imag.* 2010;26:345–354.
11. Branch KR, Busey J, Mitsumori LM, et al. Diagnostic performance of resting CT myocardial perfusion in patients with possible acute coronary syndrome. *AJR Am J Roentgenol.* 2013;200:W450–W457.
12. Meyer M, Nance JJ, Schoepf UJ, et al. Cost-effectiveness of substituting dual-energy CT for SPECT in the assessment of myocardial perfusion for the workup of coronary artery disease. *Eur J Radiol.* 2012;81:3719–3725.
13. Zhang LJ, Peng J, Wu SY, et al. Dual source dual-energy computed tomography of acute myocardial infarction: correlation with

histopathologic findings in a canine model. *Invest Radiol.* 2010;45:290–297.

14. Arnoldi E, Lee YS, Ruzsics B, et al. CT detection of myocardial blood volume deficits: dual-energy CT compared with single-energy CT spectra. *J Cardiovasc Comput Tomogr.* 2011;5:421–429.
15. Meinel FG, De Cecco CN, Schoepf UJ, et al. First-arterial-pass dual-energy CT for assessment of myocardial blood supply: do we need rest, stress, and delayed acquisition? Comparison with SPECT. *Radiology.* 2014;270:708–716.
16. Husmann L, Wiegand M, Valenta I, et al. Diagnostic accuracy of myocardial perfusion imaging with single photon emission computed tomography and positron emission tomography: a comparison with coronary angiography. *Int J Cardiovasc Imag.* 2008;24:511–518.
17. Wang R, Yu W, Wang Y, et al. Incremental value of dual-energy CT to coronary CT angiography for the detection of significant coronary stenosis: comparison with quantitative coronary angiography and single photon emission computed tomography. *Int J Cardiovasc Imag.* 2011;27:647–656.
18. Kartje JK, Schmidt B, Bruners P, et al. Dual energy CT with nonlinear image blending improves visualization of delayed myocardial contrast enhancement in acute myocardial infarction. *Invest Radiol.* 2013;48:41–45.
19. Apfaltrer P, Sudarski S, Schneider D, et al. Value of monoenergetic low-kV dual energy CT datasets for improved image quality of CT pulmonary angiography. *Eur J Radiol.* 2014;83:322–328.
20. So A, Lee TY, Imai Y, et al. Quantitative myocardial perfusion imaging using rapid kVp switch dual-energy CT: preliminary experience. *J Cardiovasc Comput Tomogr.* 2011;5:430–442.
21. Cerqueira MD, Weissman NJ, Dilsizian V, et al. Standardized myocardial segmentation and nomenclature for tomographic imaging of the heart. A statement for healthcare professionals from the Cardiac Imaging Committee of the Council on Clinical Cardiology of the American Heart Association. *Circulation.* 2002;105:539–542.
22. DeLong ER, DeLong DM, Clarke-Pearson DL. Comparing the areas under two or more correlated receiver operating characteristic curves: a nonparametric approach. *Biometrics.* 1988;44:837–845.
23. Metz CE. ROC methodology in radiologic imaging. *Invest Radiol.* 1986;21:720–733.
24. Wichmann JL, Bauer RW, Doss M, et al. Diagnostic accuracy of late iodine-enhancement dual-energy computed tomography for the detection of chronic myocardial infarction compared with late gadolinium-enhancement 3-T magnetic resonance imaging. *Invest Radiol.* 2013;48:851–856.
25. Holmes DR, Fletcher JG, Apel A, et al. Evaluation of non-linear blending in dual-energy computed tomography. *Eur J Radiol.* 2008;68:409–413.
26. Anagnostopoulos C, Georgakopoulos A, Pianou N, et al. Assessment of myocardial perfusion and viability by positron emission tomography. *Int J Cardiol.* 2013;167:1737–1749.
27. Ruzsics B, Schwarz F, Schoepf UJ, et al. Comparison of dual-energy computed tomography of the heart with single photon emission computed tomography for assessment of coronary artery stenosis and of the myocardial blood supply. *Am J Cardiol.* 2009;104:318–326.
28. Vliegenthart R, Henzler T, Moscariello A, et al. CT of coronary heart disease: part 1, CT of myocardial infarction, ischemia, and viability. *AJR Am J Roentgenol.* 2012;198:531–547.
29. Neefjes LA, Dharampal AS, Rossi A, et al. Image quality and radiation exposure using different low-dose scan protocols in dual-source CT coronary angiography: randomized study. *Radiology.* 2011;261:779–786.
30. Johansson L, Mattsson SR, Nosslin B, et al. Effective dose from radiopharmaceuticals. *Eur J Nuclear Med.* 1992;19:933–938.